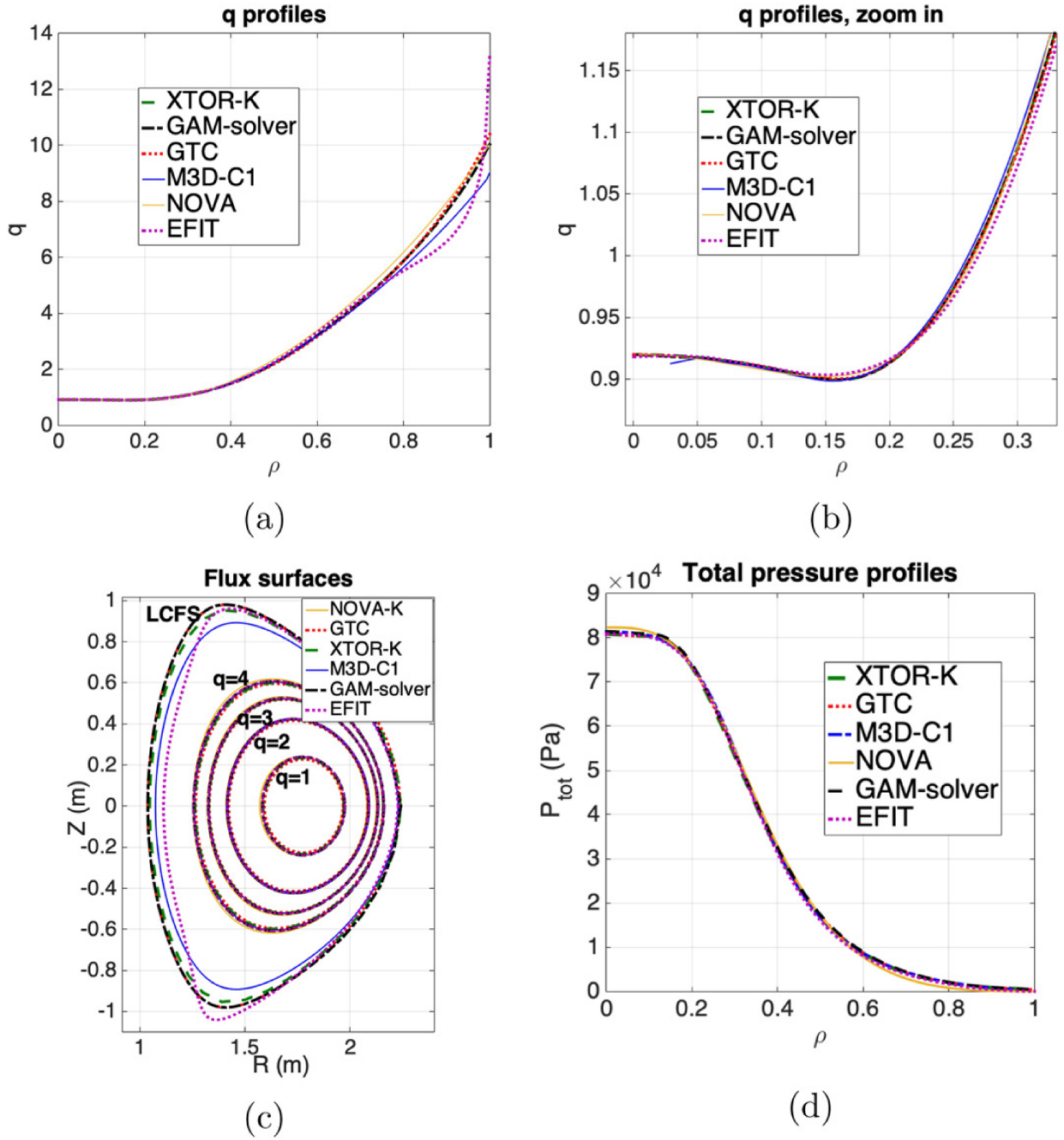
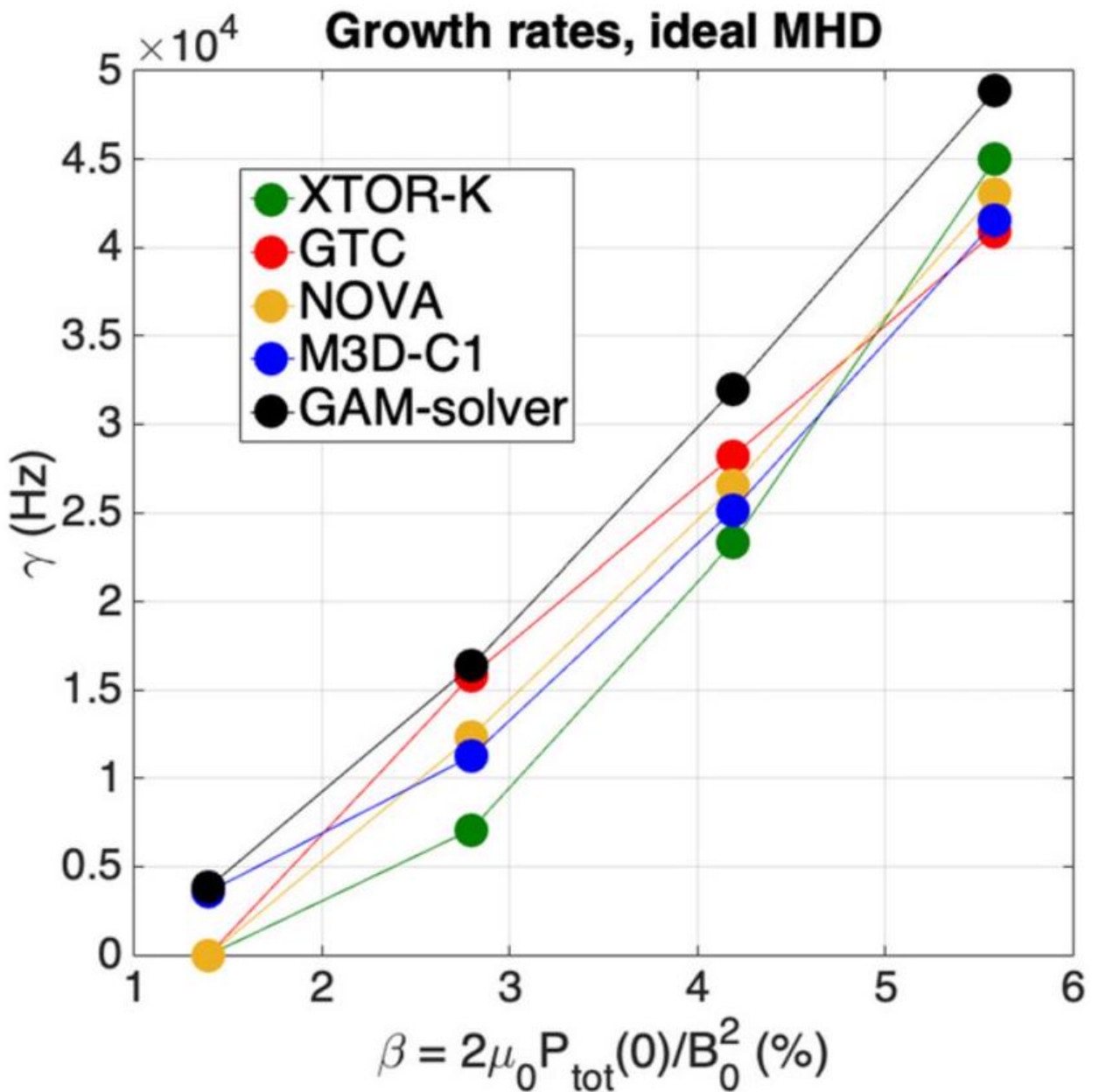


**Figure 1:** Experimental spectrogram in ms measured on the DIII-D discharge #141216. The first toroidal harmonics from  $n = 1$  to 3 are respectively displayed in black, red and blue. A clear  $n = 1$  internal kink mode appears around  $t = 1750$  ms, while a  $n = 1$  fishbone mode emerges at  $t \sim 1890$  ms.



**Figure 2:** Features of the numerical equilibria used in all codes for the kink benchmark, reconstructed from the DIII-D shot #141216 at  $t = 1750$  ms. (a) Safety factor profile (b) safety factor profile in the core. (c) Flux surfaces in the poloidal plane. (d) Total plasma pressure in Pa.



**Figure 3:** On-axis beta-scan of the internal kink growth rate obtained from the different codes, in the ideal MHD limit. An excellent quantitative agreement is obtained between codes using MHD and gyrokinetic formalisms.

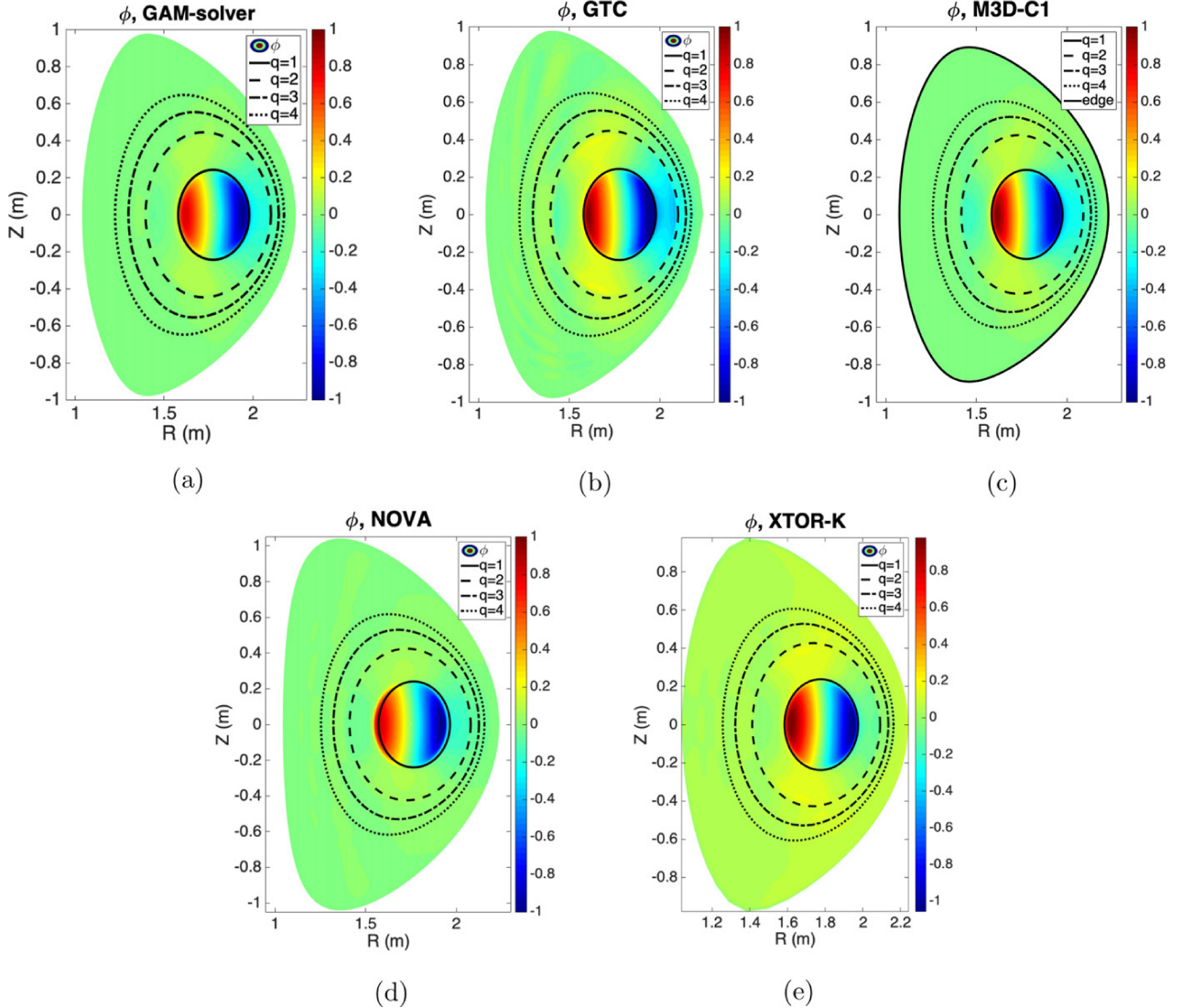


**Figure 4:** Mode structure in the poloidal plane for the electrostatic potential  $\phi$  from the different codes. The black lines correspond to the flux surfaces from  $q = 1$  to  $q = 4$ . The electrostatic potential mode structure agrees very well between all codes used in the benchmark.

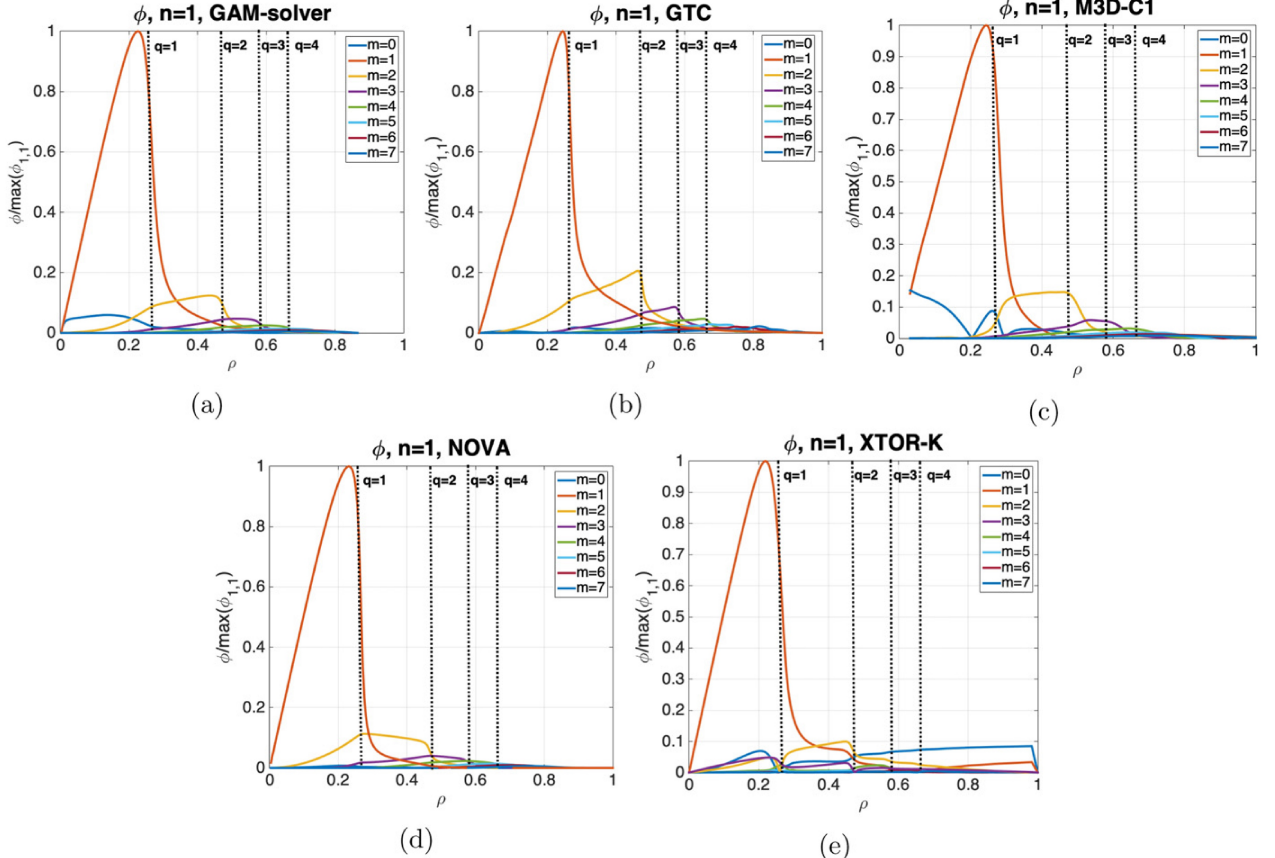


**Figure 5:** Radial mode structure of the electrostatic potential  $\phi$  obtained from the different codes for different  $m$  harmonics, as a function of the normalized toroidal flux  $\rho$ . All harmonics are normalized by the maximum value of the  $m = 1$  harmonic. The structure of the  $m = 1$  harmonic agrees very well between all codes used in the benchmark. The dashed lines correspond to the flux surfaces from  $q = 1$  to  $q = 4$ .

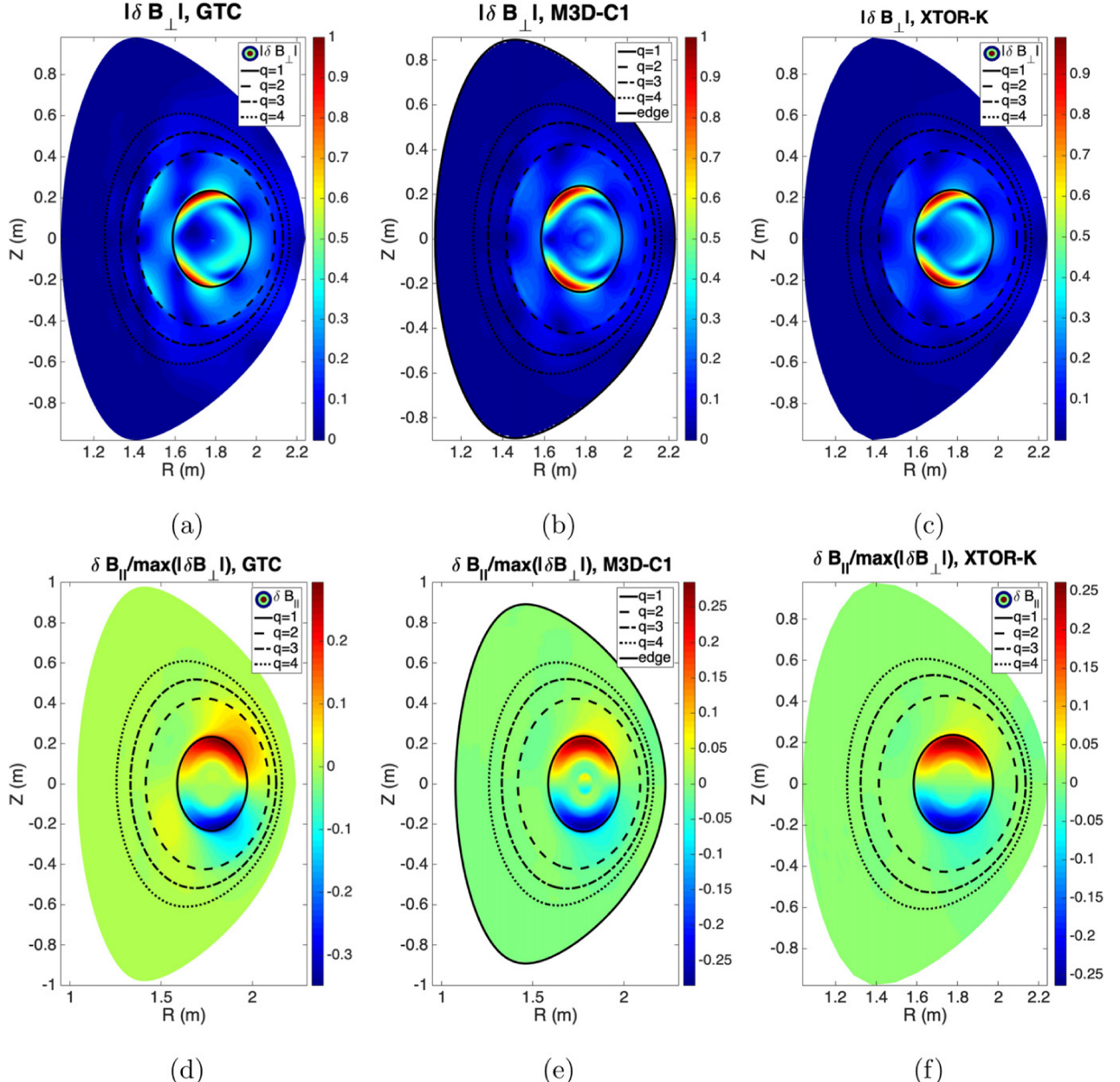


**Figure 6:** Mode structure in the poloidal plane for shear magnetic perturbation  $|\delta B_{\perp}|$  (upper panels) and compressible magnetic perturbation  $\delta B_{\parallel}/\max(|\delta B_{\perp}|)$  (lower panels) from the different codes. The black contours correspond to the flux surfaces from  $q = 1$  to  $q = 4$ .

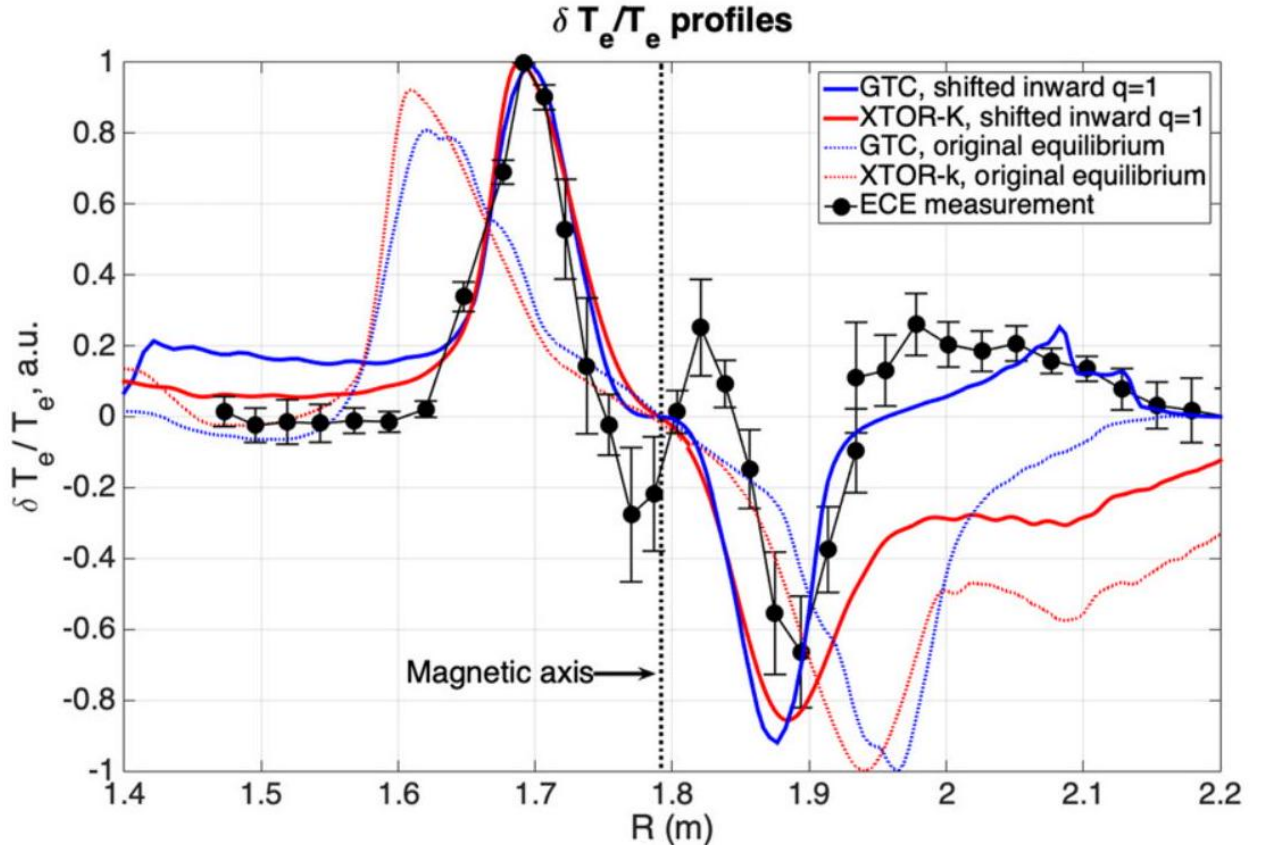


**Figure 7:** Normalized perturbed electron temperature  $\delta T_e/T_e$  against the major radius  $R$ , obtained from GTC and XTOR-K MHD simulations (blue and red lines), and from the ECE measurement of the 21kHz $n = 1$  mode (black solid circle with error bar). Dotted lines correspond to MHD simulations using the original EFIT equilibrium, and solid lines to the modified EFIT equilibrium with the  $q = 1$  flux-surface shifted inward, see figure 8 . The error bars are inferred from the random error in an ensemble of five Fourier transforms centered at 1750 ms.

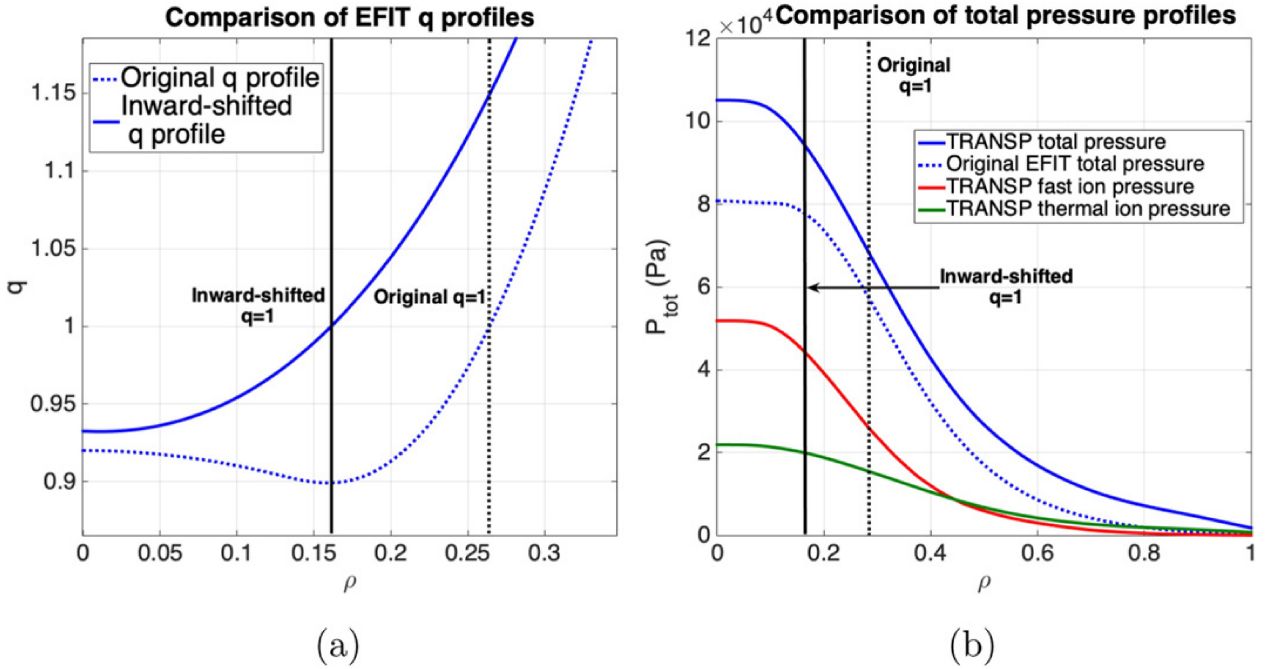


**Figure 8:** Comparison of (a) the  $q$  profiles and (b) the total pressure profiles between the original and inward-shifted EFIT reconstructions. The TRANSP total pressure is used with the inward-shifted  $q$  profile to excite the internal kink instability.

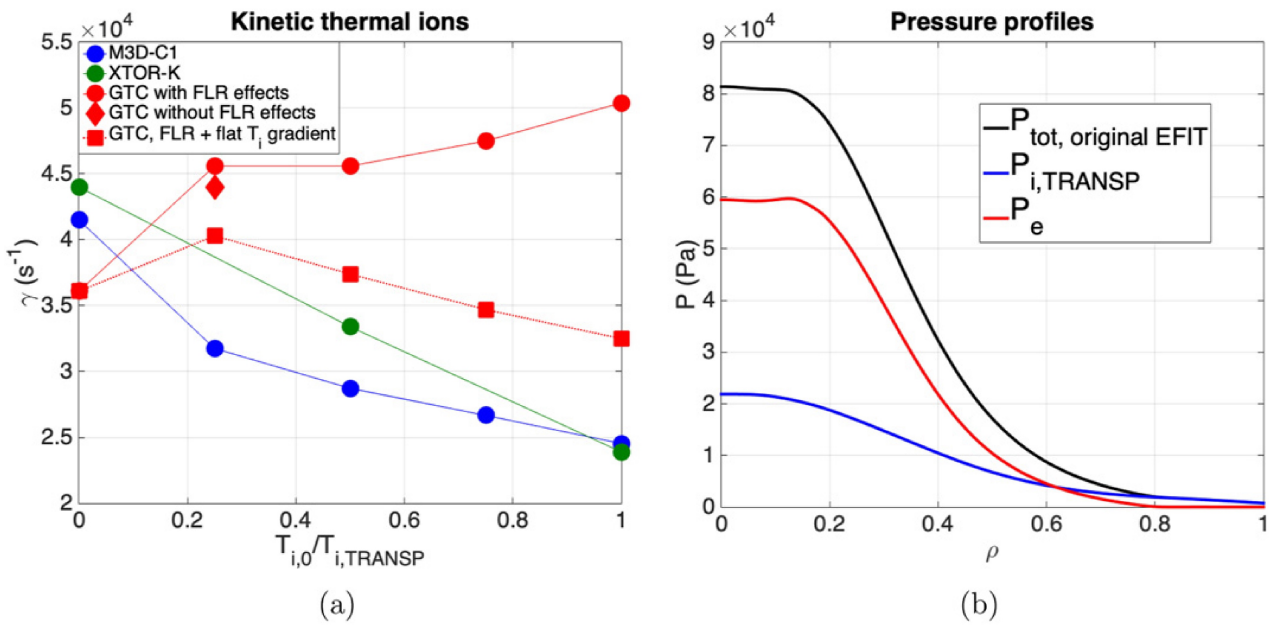


**Figure 9:** (a) Thermal ion temperature scan for the internal kink growth rate obtained from M3D-C1, XTOR-K and GTC. (b) Pressure profiles for thermal electrons and ions. The thermal ion pressure is taken from TRANSP simulations, the electron pressure profile is defined such that the sum of electron and ion pressures adds up to the total pressure obtained from original EFIT pressure.

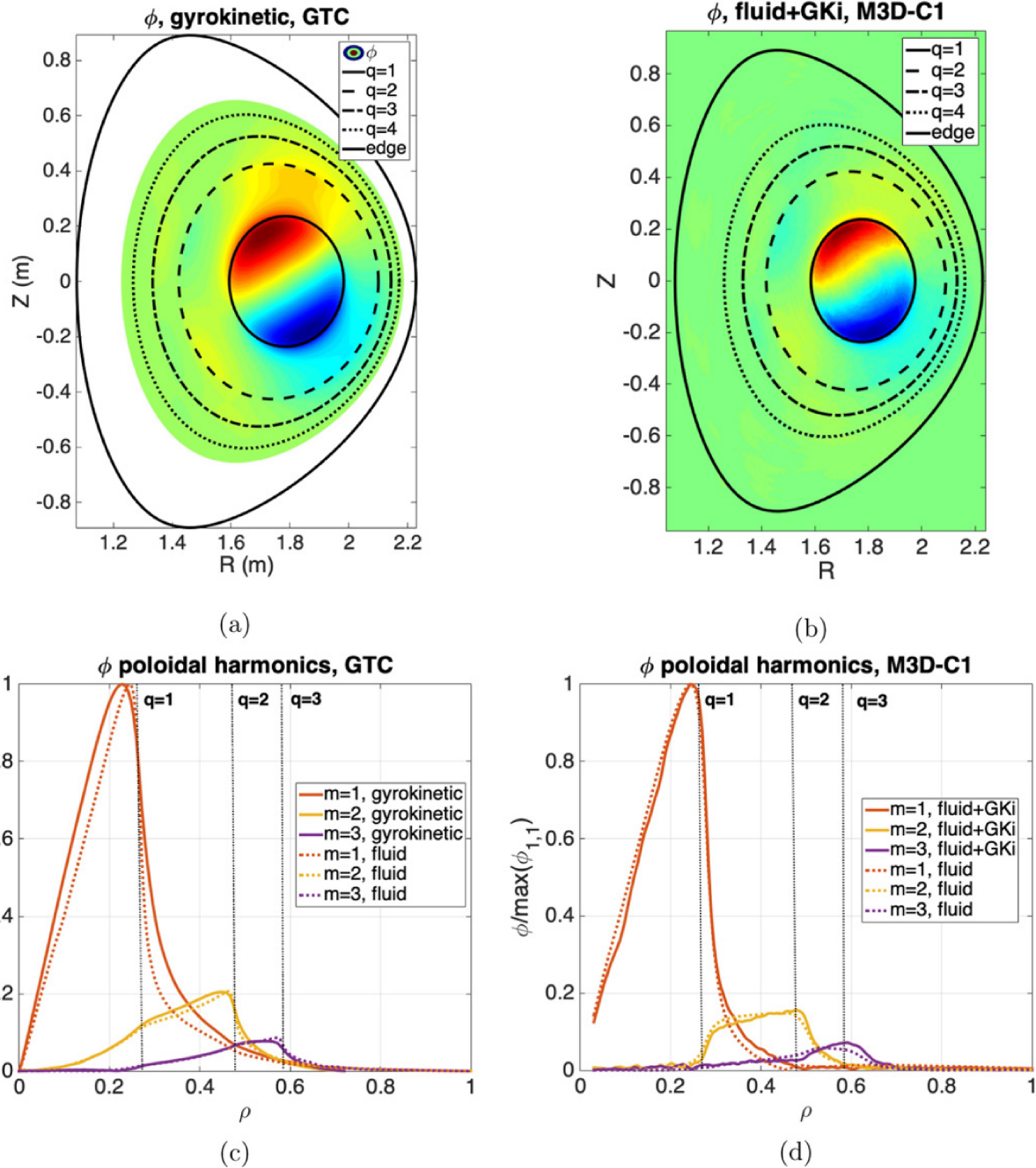


**Figure 10:** (a) and (b) Electrostatic potential of the internal kink in the poloidal plane and (c) and (d) poloidal harmonics of the  $n = 1$  electrostatic potential with gyrokinetic ions.